SUPPLEMENT

DECONSTRUCTING FACTORS CONTRIBUTING TO THE 2018 FIRE WEATHER IN QUEENSLAND, AUSTRALIA

Sophie C. Lewis, Stephanie A. P. Blake, Blair Trewin, Mitchell T. Black, Andrew J. Dowdy, Sarah E. Perkins-Kirkpatrick, Andrew D. King, and Jason J. Sharples

This document is a supplement to "Deconstructing Factors Contributing to the 2018 Fire Weather in Queensland, Australia," by Sophie C. Lewis, Stephanie A. P. Blake, Blair Trewin, Mitchell T. Black, Andrew J. Dowdy, Sarah E. Perkins-Kirkpatrick, Andrew D. King, and Jason J. Sharples (*Bull. Amer. Meteor. Soc.*, **101**, S115–S122) • ©2020 American Meteorological Society • *Corresponding author:* Sophie C. Lewis, s.lewis@adfa.edu.au • DOI:10.1175/BAMS-D-19-0144.2

OBSERVATIONS. Daily temperature (T_{max} and T_{min}; °C) and precipitation (% of mean) anomalies were taken from the Australian Water Availability Project (AWAP) gridded data (Jones et al. 2009) (relative to 1910–218 climatology). We present temperatures for November and the conditioning heatwave event (24–29 November) and precipitation for spring [September–November (SON)]. Gridded McArthur Forest Fire Danger Index (FFDI) data were calculated by Dowdy (2018) using winds derived from reanalysis and observed rainfall and temperature. Mean monthly FFDI values (from 1979) and count of days > 99th percentile in each month were used (from 1950). Mean sea level pressure (MSLP; hPa), relative humidity (RH; %) at 850 hPa, and 10-m wind speed (m s^{-1}) and direction were derived from ERA-Interim (from 1979) (Dee et al. 2011). Large-scale modes of variability [the southern annular mode (SAM), El Niño–Southern Oscillation (ENSO) and Indian Ocean dipole (IOD)] are assessed using SAM, Niño-3.4, and Dipole Mode Index (DMI) indices.

CMIP5. Model temperature (tas) and precipitation (pr) data from CMIP5 (Taylor et al. 2012) historical, historicalNat, and RCP8.5 experiments were examined for November temperatures in the fire region and SON precipitation in QLD. Models were selected based on performance and examined as described by Lewis and Karoly (2014). Risk ratios (RRs) associated with anthropogenic forcings were calculated by comparing the probability of exceeding observed 2018 anomalies in RCP8.5 experiments (years 2006–35) with historicalNat (all years). Very likely RR (>90%) values (see Lewis and Karoly 2013) are provided. Table ES1 shows models, experiments, and years analyzed.

WEATHER@HOME. Model data from the weather@home Australia–New Zealand project (Black et al. 2016) were used to examine mean temperature, precipitation, MSLP, RH, and winds. As 2018 data are not yet available, we use simulations driven by time-evolving sea surface fields created by compositing selected historical El Niño episodes [see Black (2017) for details]. As an analog to 2018, we use neutral ENSO condition simulations and we compare variables in ALL scenarios (present-day atmospheric composition) with NAT scenarios (preindustrial atmospheric composition and composited surface field modified by removing nine different anthropogenic response pattern estimates, delta-SST).

The ALL simulation uses atmospheric compositions (greenhouse gases (CO_2, CH_4, and N_{20}), ozone, halocarbons, sulfur species) and solar anomalies specific for CMIP5 with post-2005 greenhouse gas concentrations and aerosol emissions following the RCP8.5 scenario. The NAT simulation delta-SST estimates are calculated from CMIP5 models as the decadal-average (1996–2005) SSTs from the historical simulations minus the corresponding historicalNat simulations. The NAT simulations have prescribed preindustrial (1850) levels of greenhouse gases, ozone,

and aerosols, and sea ice extent is the maximum observed in each hemisphere, compared for ALL and NAT. Hence, model anomalies (ALL – NAT) span a more substantial forcing than in observations (1911–2018) and not directly comparable. We have not conducted an evaluation of the simulations for the Queensland region and instead rely on previous work that found the model resolves key climatic features in Australia and provides good representations of spatial and temporal variability of temperature and precipitation (Black et al. 2016).

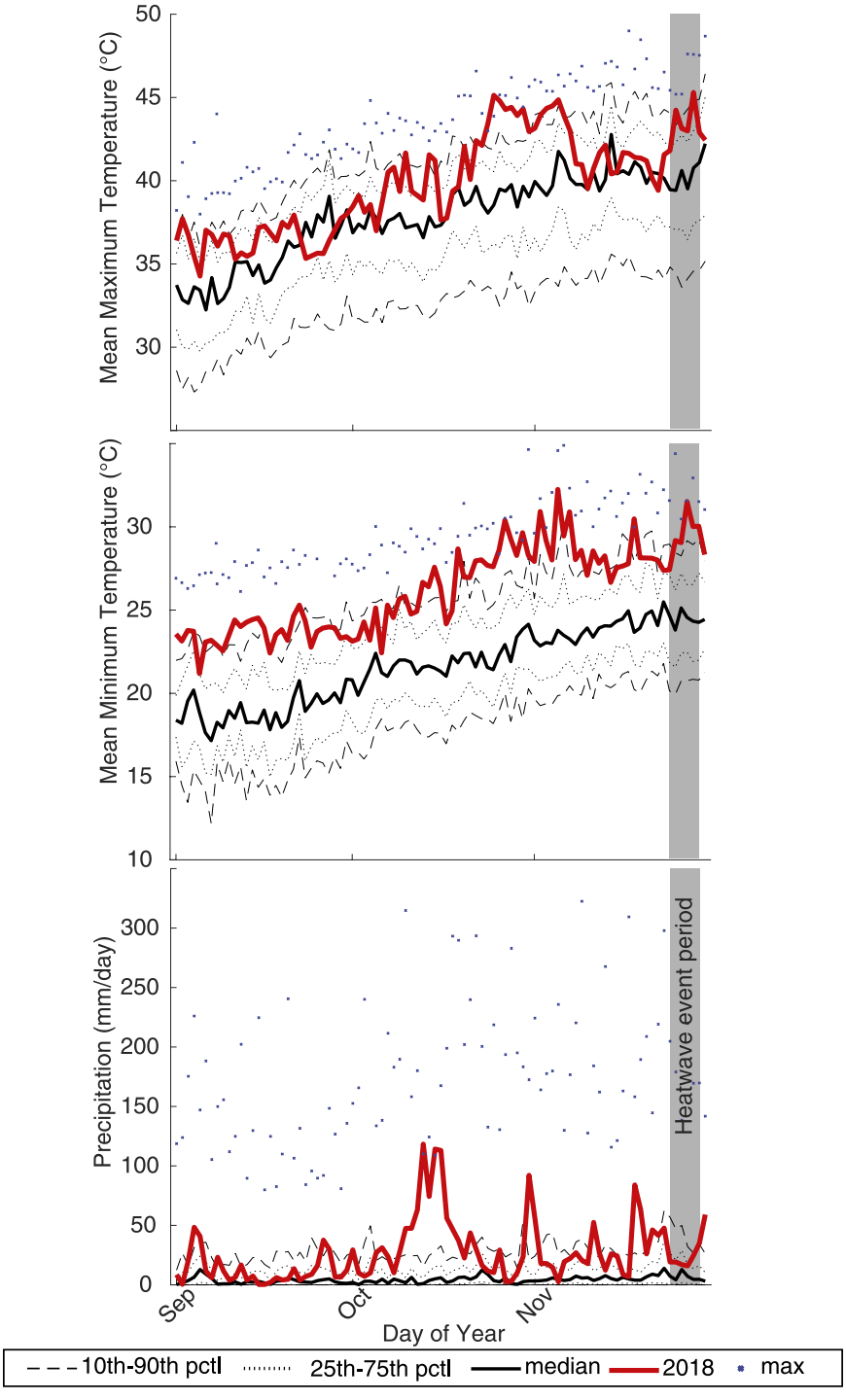

Fig. ES1. Observed Queensland area-average (a) T_{max}, (b) T_{min}, and (c) precipitation for each day of the spring (SON) period composited from long-term (1911–2018 data). Plots show the area-averaged 10th–90th (dashed line) and 25th–75th (dotted line) percentile, median (black line), daily maximum (plot squares), and 2018 mean (red line). Horizontal gray bars show the 2018 heatwave period (24–29 Nov), demonstrating the event was particularly notable for extreme T_{min} values.

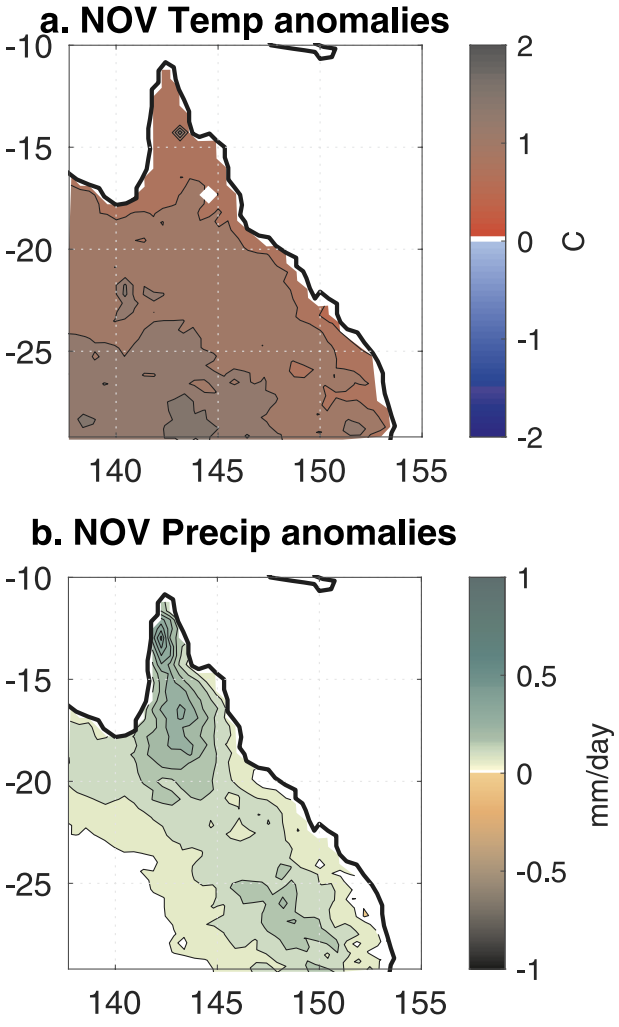

Fig. ES2. Comparison of ALL and NAT weather@home ensembles for ensembles composites for (a) temperature anomalies (°C) (ALL − NAT) and (b) precipitation (mm day^{-1}).

Table ES1. CMIP5 experiments, models, and realizations used and number of realizations for weather@home.

CMIP5

tas	Realizations analyzed			pr	Realizations analyzed		
Models analyzed	Historical (1976–2005)	Historical-Nat (1850–2005)	RCP8.5 (2006–35)	Models analyzed	Historical (1976–2005)	Historical-Nat (1976–2005)	RCP8.5 (2006–35)
BNU-ESM	1	1	1	CESM1-CAM5	3	3	3
CESM1-CAM5	3	3	2	CanESM2	5	5	5
CanESM2	5	5	2	GFDL CM3	5	3	1
GFDL CM3	5	3	1	GISS-E2-H	18	10	5
HadGEM2-ES	5	4	4	HadGEM2-ES	5	4	4
MIROC-ESM-CHEM	1	1	1	IPSL-CM5A-MR	3	3	4
NorESM1-M	3	1	1	MIROC-ESM-CHEM	1	1	1
CNRM-CM5	10	6	6	NorESM1-M	3	1	1
GFDL-ESM2M	1	1	1	CCSM4	8	4	4
GISS-E2-R	26	8	5	CNRM-CM5	10	6	6
MIROC-ESM	3	3	1	GFDL-ESM2M	1	1	1
MRI-CGCM3	5	1	1	GISS-E2-R	26	10	5
BCC-CSM1.1	3	1	1	MIROC-ESM	3	3	1
				MRI-CGCM3	5	1	1
				BCC-CSM1.1	3	1	1

weather@home

Realizations analyzed		
Variable	ALL	NAT
Temperature	1655	1899
Precipitation	1655	1899
MSLP	1655	1899
Humidity	1655	1899